LAWRENCE
LIVERMORE
NATIONAL
LABORATORY

LLNL-TR-404055

Surface-pressure Tides Simulated by WACCM-1 and CMIP3 / IPCC Climate Models

Curt Covey, Aiguo Dai, Richard S. Lindzen

May 21, 2008

Disclaimer

This work performed under the auspices of the U.S. Department of Energy by Lawrence Livermore National Laboratory under Contract DE-AC52-07NA27344.

curtcovey@yahoo.com

Surface-pressure Tides Simulated by WACCM-1 and CMIP3 / IPCC Climate Models

Curt Covey, Aiguo Dai and Richard S. Lindzen
20 May 2008

Atmospheric tides driven by solar heating are readily detectable at Earth's surface (Hagan et al. 2003). In the middle and upper atmosphere they attain large amplitudes and can be the most significant part of atmospheric motion. Output from the Whole-Atmosphere Community Climate Model (WACCM), a general circulation model extending from the surface to the thermosphere, contains tidal oscillations in the middle and upper atmosphere (Richter et al. 2008 **?**). Here we examine the surface-pressure signature of the tides in output from both WACCM and the climate models contributing to the IPCC 4th Assessment Report (Randall et al. 2007). We compare these simulations with the most recent and complete set of surface pressure observations (Dai and Wang 1999).

All of the model output we analyze is publicly available. The WACCM output is from an early version of the model (WACCM-1; Sassi et al. 2002) and was downloaded from NCAR's Community Data Portal (http://cdp.ucar.edu). The IPCC output was taken from archives of the Coupled Model Intercomparison Project, phase 3 (CMIP3; see Meehl et al. 2007) on the PCMDI's Earth System Grid portal (http://esg.llnl.gov/portal).

Our starting point for global analysis of WACCM output is 3-hourly surface pressure data, expressed for each day and grid point as anomalies about that day's and grid point's mean value. Fourier analysis in the time dimension shows that the dominant frequency of the surface-pressure tides is twice a day (semidiurnal) rather than once a day (diurnal) in both the observations and the model:

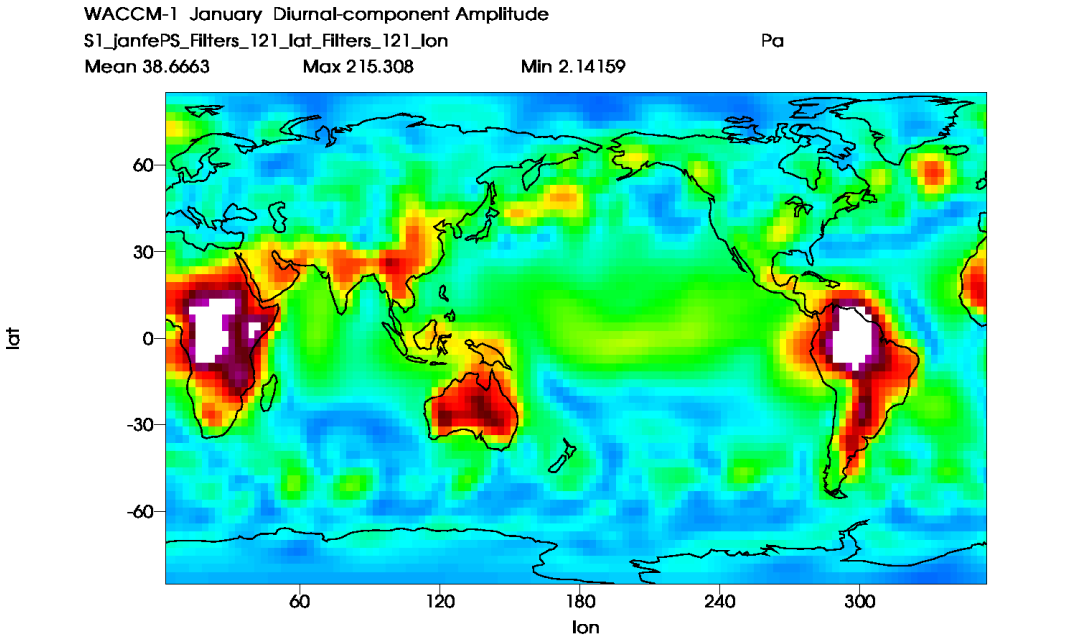
WACCM-1 January Diurnal-component Amplitude
S1_janfePS_Filters_121_lat_Filters_121_lon
Pa
Mean 38.6663
Max 215.308
Min 2.14159
lat
60
30
0
-30
-60
60
120
180
240
300
lon
0
20
40
60
80
100
120
140
160

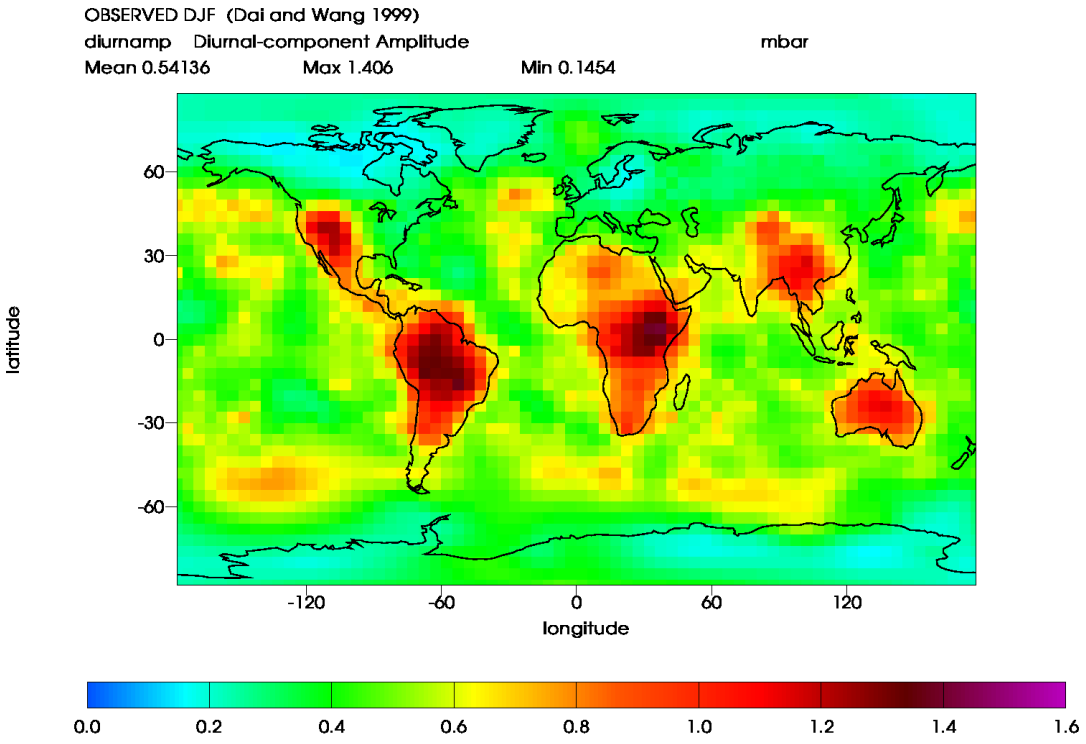
OBSERVED DJF (Dai and Wang 1999)
diurnamp Diurnal-component Amplitude
mbar
Mean 0.54136
Max 1.406
Min 0.1454
latitude
60
30
0
-30
-60
-120
-60
0
60
120
longitude
0.0
0.2
0.4
0.6
0.8
1.0
1.2
1.4
1.6

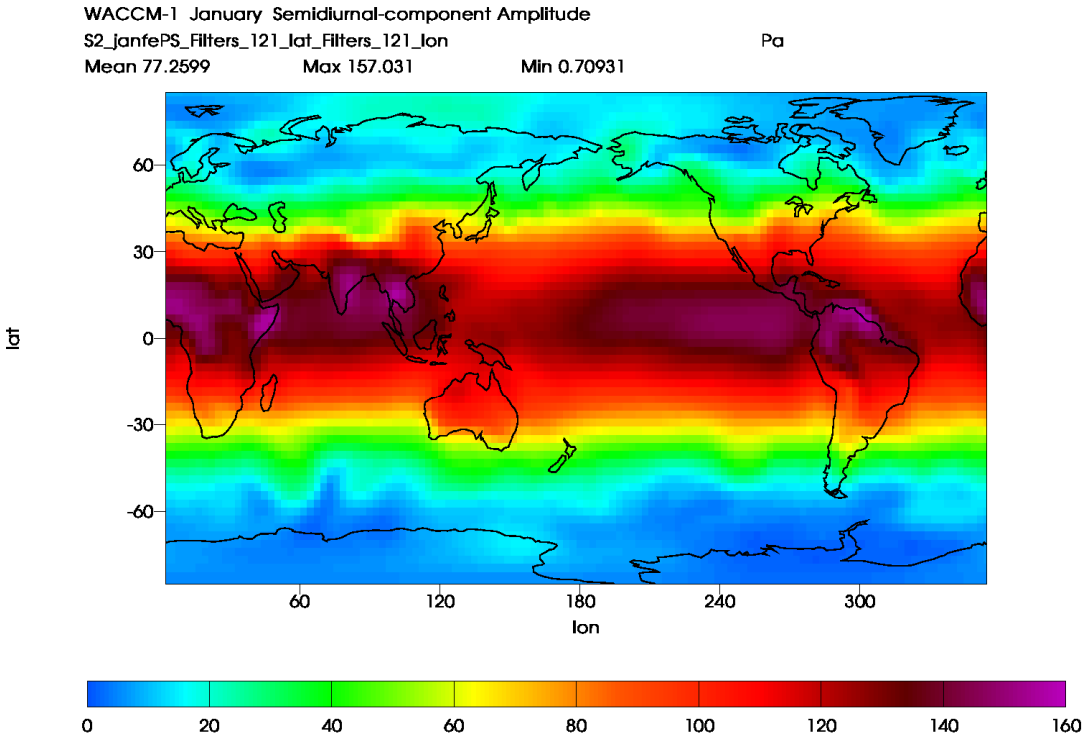
WACCM-1 January Semidiurnal-component Amplitude
S2_janfePS_Filters_121_lat_Filters_121_lon
Pa
Mean 77.2599
Max 157.031
Min 0.70931
lat
60
30
0
-30
-60
60
120
180
240
300
lon
0
20
40
60
80
100
120
140
160

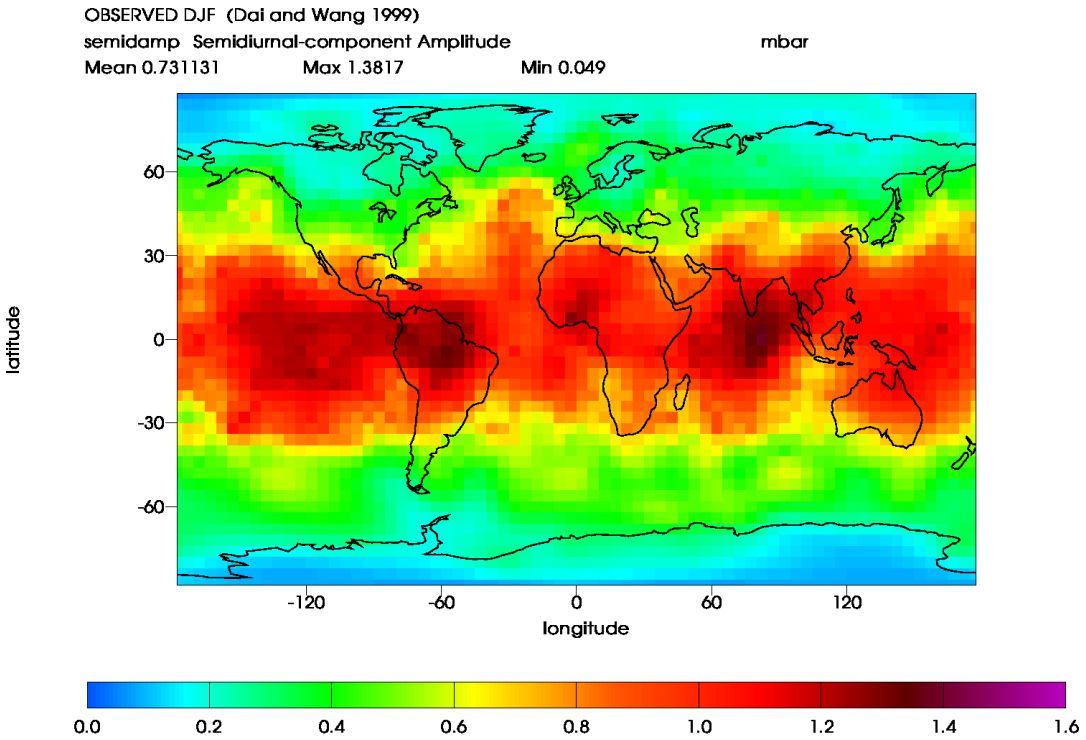
OBSERVED DJF (Dai and Wang 1999)
semidamp Semidiurnal-component Amplitude
mbar
Mean 0.731131
Max 1.3817
Min 0.049
latitude
60
30
0
-30
-60
-120
-60
0
60
120
longitude
0.0
0.2
0.4
0.6
0.8
1.0
1.2
1.4
1.6

In addition to capturing the dominance of the semidiurnal component, WACCM agrees with observations that diurnal tide amplitudes are much stronger in some continental regions than they are in ocean areas, while semidiurnal tide amplitude is nearly independent of longitude. There is also qualitative model-observed agreement that tidal amplitudes decrease from Equator to Pole. Quantitatively, the model overpredicts diurnal amplitude by up to 50% and semidiurnal amplitude by 5 – 10 %.

The phase of the tides equatorward of ~ 30 degrees latitude (where amplitudes are significant) puts the diurnal pressure maximum at about 6 AM local solar time and the semidiurnal pressure maximum at about 10 AM and PM local solar time, in both the model and observations:

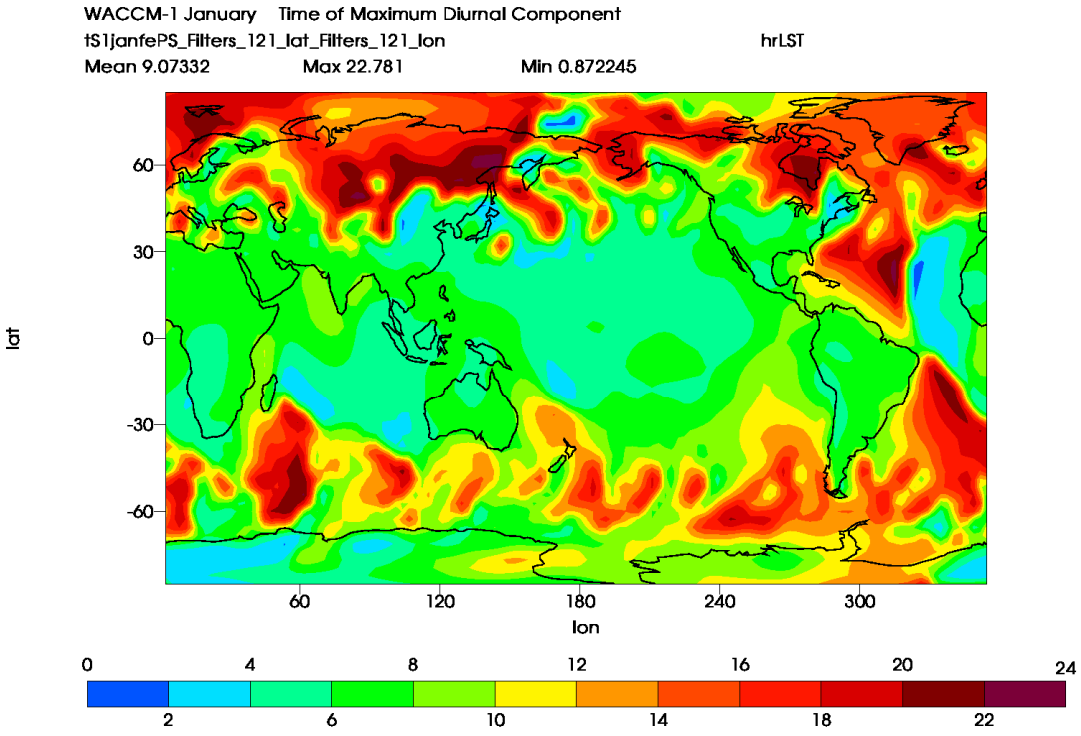
WACCM-1 January Time of Maximum Diurnal Component
tS1janfePS_Filters_121_lat_Filters_121_lon
hrLST
Mean 9.07332
Max 22.781
Min 0.872245
lat
60
30
0
-30
-60
60
120
180
240
300
lon
0
4
8
12
16
20
24
2
6
10
14
18
22

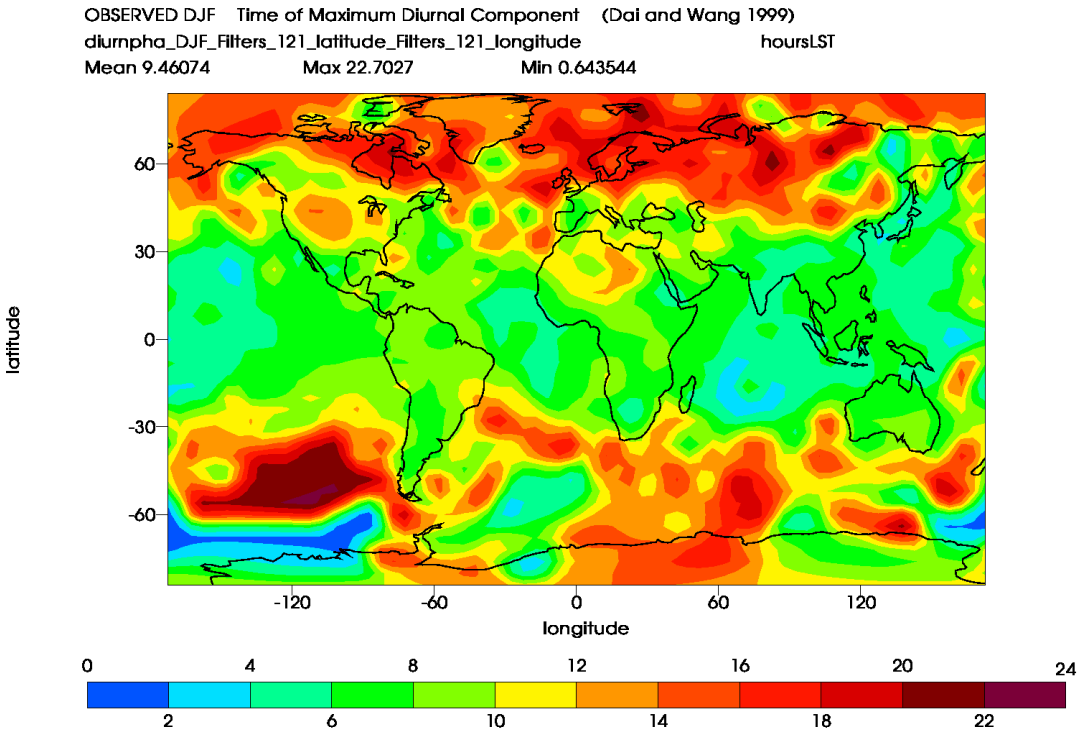
OBSERVED DJF Time of Maximum Diurnal Component (Dai and Wang 1999)
diurnpha_DJF_Filters_121_latitude_Filters_121_longitude
hoursLST
Mean 9.46074
Max 22.7027
Min 0.643544
latitude
60
30
0
-30
-60
-120
-60
0
60
120
longitude
0
4
8
12
16
20
24
2
6
10
14
18
22

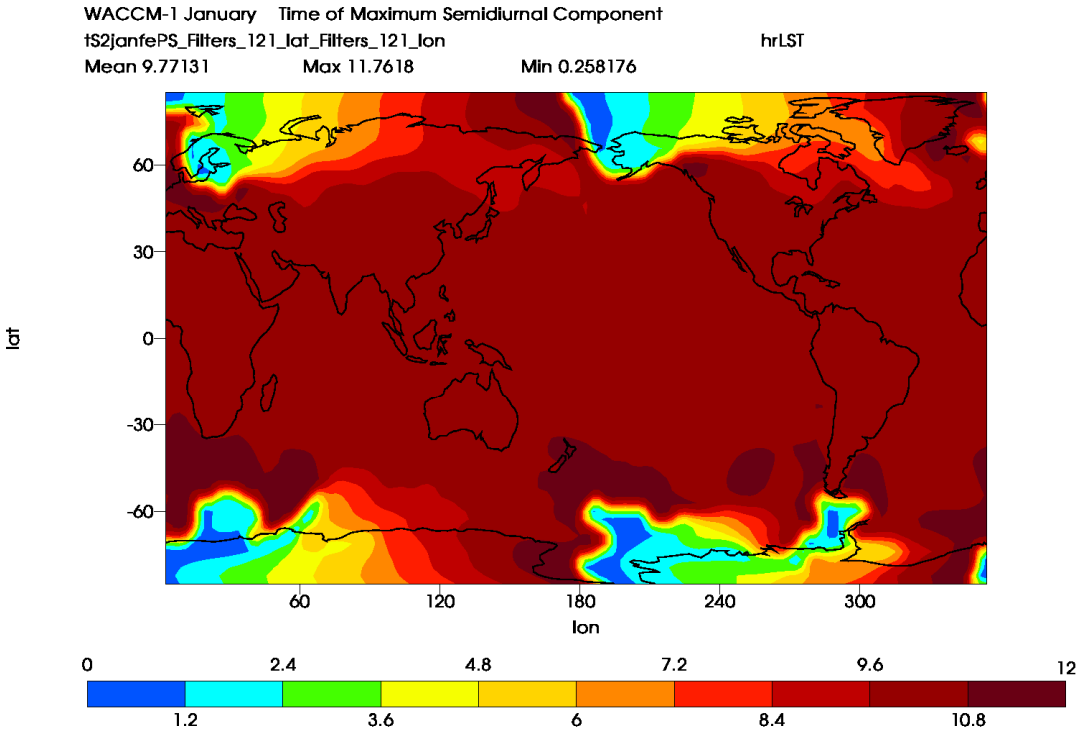
WACCM-1 January Time of Maximum Semidiurnal Component
tS2janfePS_Filters_121_lat_Filters_121_lon hrLST
Mean 9.77131 Max 11.7618 Min 0.258176
lat
60
30
0
-30
-60
60
120
180
240
300
lon
0
2.4
4.8
7.2
9.6
12
1.2
3.6
6
8.4
10.8

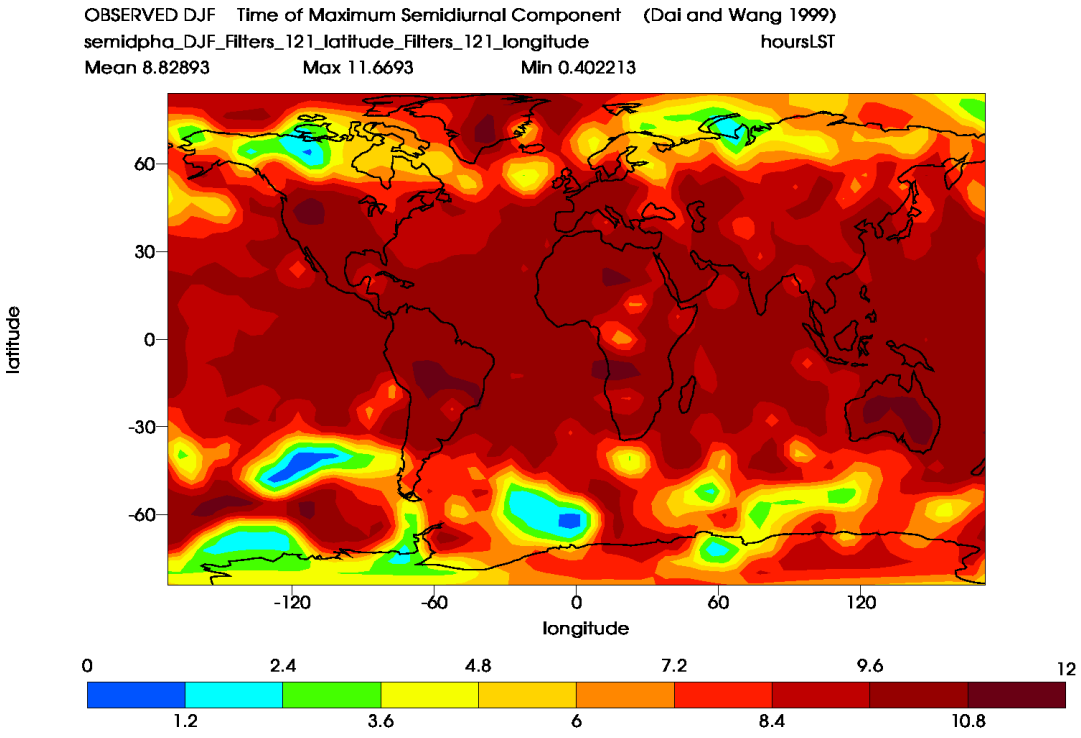
OBSERVED DJF Time of Maximum Semidiurnal Component (Dai and Wang 1999)
semidpha_DJF_Filters_121_latitude_Filters_121_longitude hoursLST
Mean 8.82893 Max 11.6693 Min 0.402213
latitude
60
30
0
-30
-60
-120
-60
0
60
120
longitude
0
2.4
4.8
7.2
9.6
12
1.2
3.6
6
8.4
10.8

More precise information about the speed and direction of tide propagation comes from an additional Fourier analysis in the longitude (zonal) dimension. Using Dai and Wang's algorithms, we obtain the following result for the semidiurnal component of WACCM's simulation:

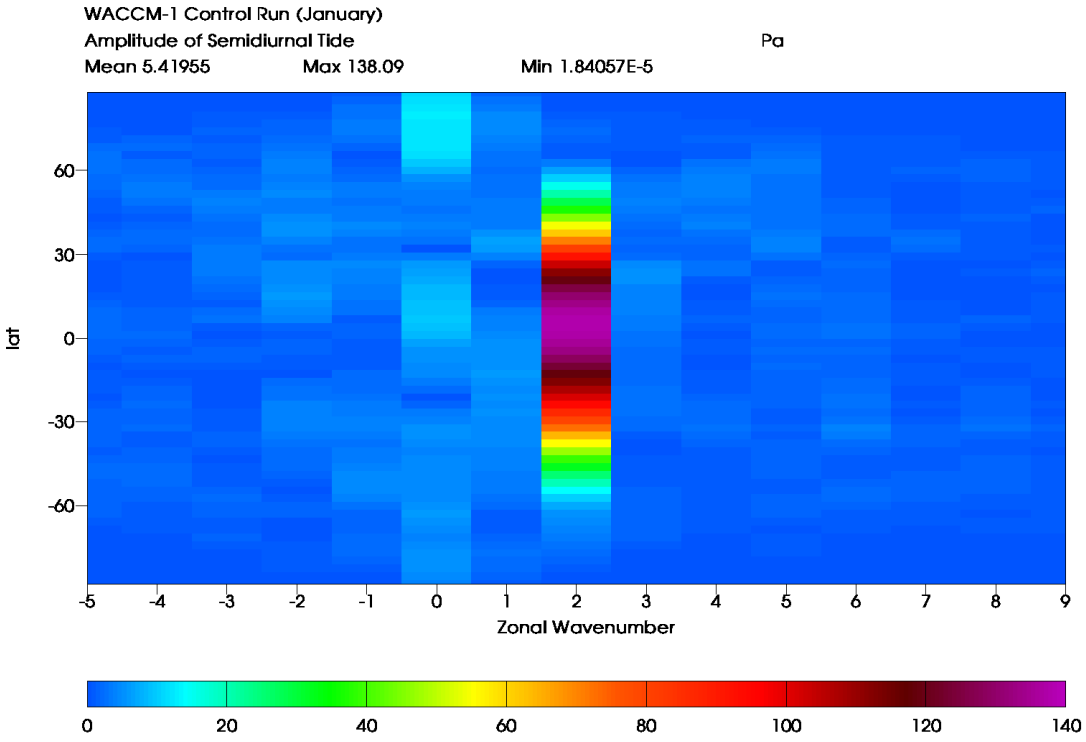

This result should be compared with the observations shown in Dai and Wang's Figure

14, displayed below in the same format as our WACCM figure:

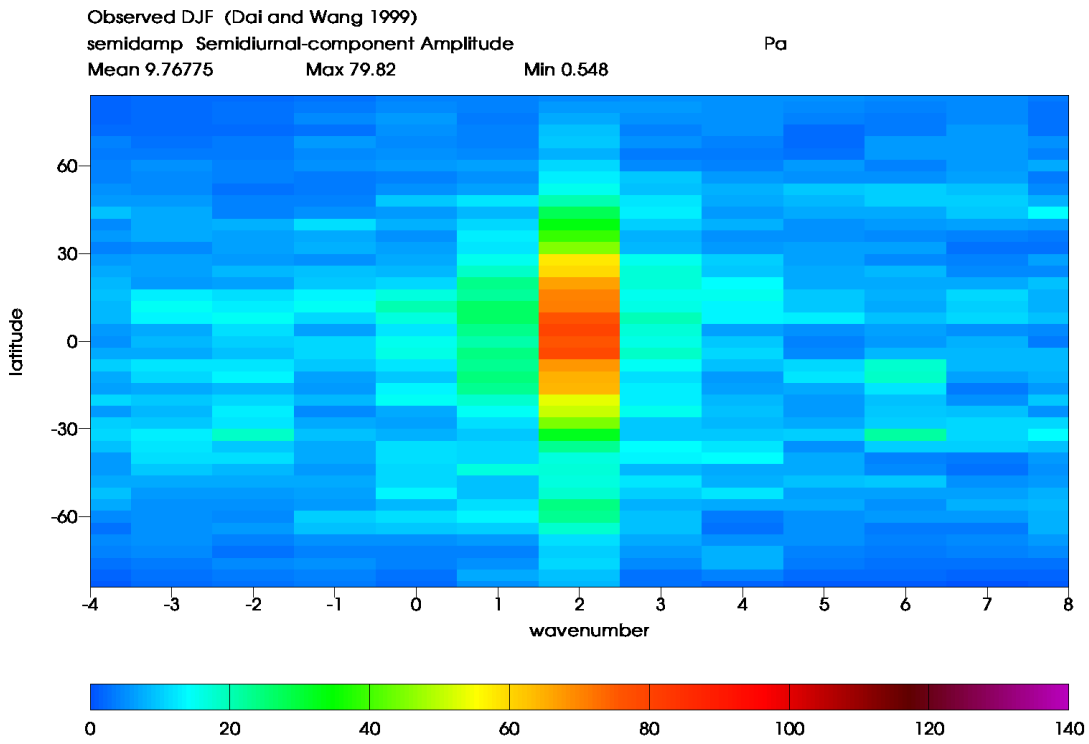

Qualitatively, simulation and observation agree that equatorward of ~ 45 degrees latitude, most of the semidiurnal amplitude appears at zonal wavenumber 2. This component of the tide migrates eastward in step with the apparent motion of the Sun across the sky. (The amplitude is proportional to $\exp[i (s \lambda + 2\pi n t / T)]$ with λ = east longitude, t = time, T = 24 hours, and $s = n = 2$.) Quantitative comparison, however, reveals that the model puts too much amplitude into wavenumber 2 and too little amplitude into other wavenumbers. WACCM's peak wavenumber 2 amplitude is nearly 140 Pa, compared with less than 70 Pa observed.

Similarly, for the diurnal component we have the following:

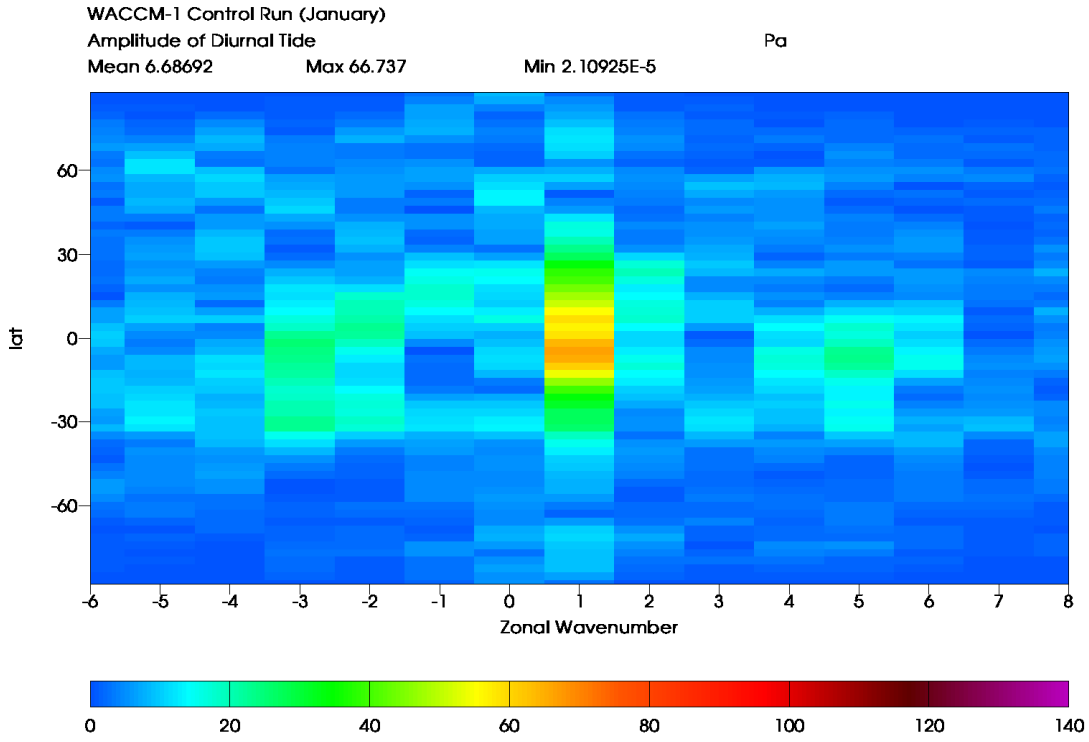
WACCM-1 Control Run (January)
Amplitude of Diurnal Tide
Pa
Mean 6.68692
Max 66.737
Min 2.10925E-5
lat
60
30
0
-30
-60
-6
-5
-4
-3
-2
-1
0
1
2
3
4
5
6
7
8
Zonal Wavenumber
0
20
40
60
80
100
120
140

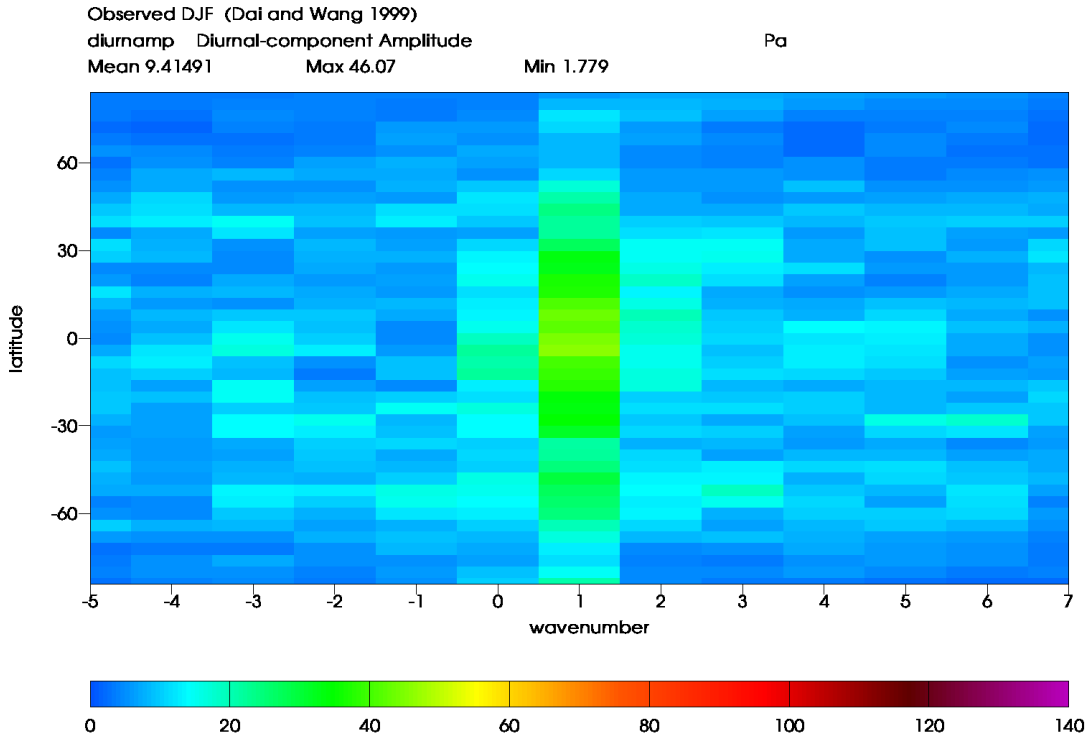

Again the main component migrates with the Sun ($s = n = 1$) but is overrepresented in the model.

We now consider the CMIP3 / IPCC model output. Nine contributions to the CMIP3 database included high-frequency (3-hourly) output of *sea-level* pressure from coupled ocean-atmosphere simulations of the 20th century. Unfortunately, the database does not contain high-frequency output of *surface* pressure. The two are of course identical for ocean areas but can differ significantly over land.

Six of the nine models also provided high-frequency output of a single year (2000) from atmosphere-only simulations using observed sea surface temperatures and sea ice concentrations (i.e., AMIP simulations). At the time we extracted the data (2007-2008) three of the models had a simple error in the time-coordinate values recorded for CMIP3. After consulting the model developers, we added 1.5 hours to GISS-EH and GISS-ER times, and we subtracted 4.5 hours from INM-CM3.0 times, to correct these errors.

The table below shows our first screening test of the CMIP3 / IPCC output and comparison with both sea-level and surface pressure output from WACCM:

Air-pressure Tides Near "Batavia" (now Jakarta): 14°S-2°N, 97.5°E-112.5°E

Source*			Diurnal component		Semidiurnal component	
	Top of model	Str+ levs**	Amplitude [mbar]	Time of max [LST]	Amplitude [mbar]	Time of max [LST]
CNRM-CM3	0.05 mb	20	0.7165	4:35	1.4010	9:35
CNRM-CM3 AMIP			0.7601	4:42	1.3762	9:38
GFDL-CM2.0	3.00 mb	4	0.4402	6:16	1.3455	10:22
GFDL-CM2.1	3.00 mb	4	0.6095	5:46	1.3112	10:39
GISS-EH	0.10 mb	10	0.7039	4:15	1.7625	10:35
GISS-ER	0.10 mb	10	0.9469	4:19	1.8195	10:33
GISS-ER AMIP			0.7762	4:54	1.7533	10:09
INM-CM3.0	10.00 mb	7	0.6513	5:08	1.4486	10:04
INM-CM3.0 AMIP			0.7378	3:47	1.4763	10:03
MIROC3.2(hi-res)	40 km	22	0.4043	6:16	1.4801	10:09
MIROC3.2(hi-res) AMIP	≈ 3 mb		0.5774	6:31	1.4452	10:11
MIROC3.2(med-res)	30 km	6	0.6403	6:60	1.7809	10:54
MIROC3.2(med-res)AMIP	≈ 10 mb		0.6238	7:34	1.6323	10:52
MRI-CGCM3.2	0.40 mb	7	0.5923	5:46	1.9330	11:14
MRI-CGCM3.2 AMIP			0.4899	5:38	1.7558	10:57
WACCM-1 Jan climat PS	3×10^{-6} mb	51	0.5205	5:17	1.2520	10:48
WACCM-1 Jan climat PSL			0.5491	5:12	1.2599	10:48
WCCAM-1 Jul climat PS			0.5709	3:15	1.1361	10:48
WCCAM-1 Jul climat PSL			0.5945	3:17	1.1428	10:47
OBSERVATIONS			0.6491	5:59	0.9984	9:56

*Observations are from Dai and Wang (1999) for the September – October – November season of years 1976-1997. Simulations are for the first half of November (unless otherwise labeled) in the first year of high-frequency model output (1991 for all CMIP3 models except INM-CM3.0, in which the first year is 2000) corresponding to the "classic" observation described in the text. All models use a coupled atmosphere – land surface – ocean – sea ice GCM with realistic late-20th century forcing (time-varying greenhouse gas and aerosol amounts, time-varying solar energy input, etc.) except for sources labeled "AMIP" or "control." AMIP simulations force an atmospheric GCM with sea surface temperatures and sea ice concentrations observed for the period 1979 – present; climatology runs force with a repeating climatological-average seasonal cycle of SST and sea ice. Shaded and unshaded rows are used to distinguish different atmospheric GCMs. For CMIP3 model information, see Table 8.1 in Randall et al. (2007) and references therein. For WACCM-1 model information, see Sassi et al. (2002). Observations are of surface pressure. Available model output is sea-level pressure from CMIP3, both sea-level and surface pressure (PS) from WACCM-1.

**Number of model levels in or above the stratosphere, defined here as altitudes > 15 km or pressure-levels < 150 mbar.

We took an area average of sea-level pressure in the vicinity of Batavia (now Jakarta), Indonesia, from both the models and observations. The classic signature of the tides—shown in Figure 1.1 of Chapman and Lindzen (1970)—is a twice-daily or "semidiurnal" variation of surface pressure. Chapman and Lindzen's figure shows data taken at Batavia during the first half of November 1919; the observed amplitude is ±1-1.5 mbar and the observed phase puts maxima at about 10 AM and 10 PM Local Solar Time. Dai and Wang's observations confirm that the "Batavia" measurements are representative of tropical ocean areas in all seasons.

Using the table to compare simulations with the recent observations, we see that all of the models obtain roughly the correct diurnal and semidiurnal amplitudes and phases at Batavia. Comparing results from the coupled ocean-atmosphere 20th century simulations with results from the AMIP simulations shows close agreement. For each model that provided an AMIP simulation, the difference between it and the coupled ocean-atmosphere simulation is 10% or less in amplitude, and 17 minutes or less in phase, for the dominant semidiurnal component of the tide. We conclude that the tide simulations are not sensitive to errors in model-computed SST and sea ice amounts, or to chaotic "weather" effects. In what follows we use only output from the CMIP3 / IPCC 20th century simulations.

As with WACCM, our starting point for global analysis of model output is the complete set of available 3-hourly pressure data, expressed for each day and grid point as anomalies about that day's and grid point's mean value. The GISS and MIROC3.2 medium-resolution models provided 10 simulated years of 3-hourly data, GFDL-CM2.0 provided 5 years, MIROC3.2 high-resolution provided 2 years, and all others provided 1 year. As a qualitative screening test, we examined the final two days of each time series. Animations (not shown) clearly reveal low-latitude wavenumber-2 disturbances propagating westward with the Sun's apparent motion across the sky. The following maps show one time point from each model's animation:

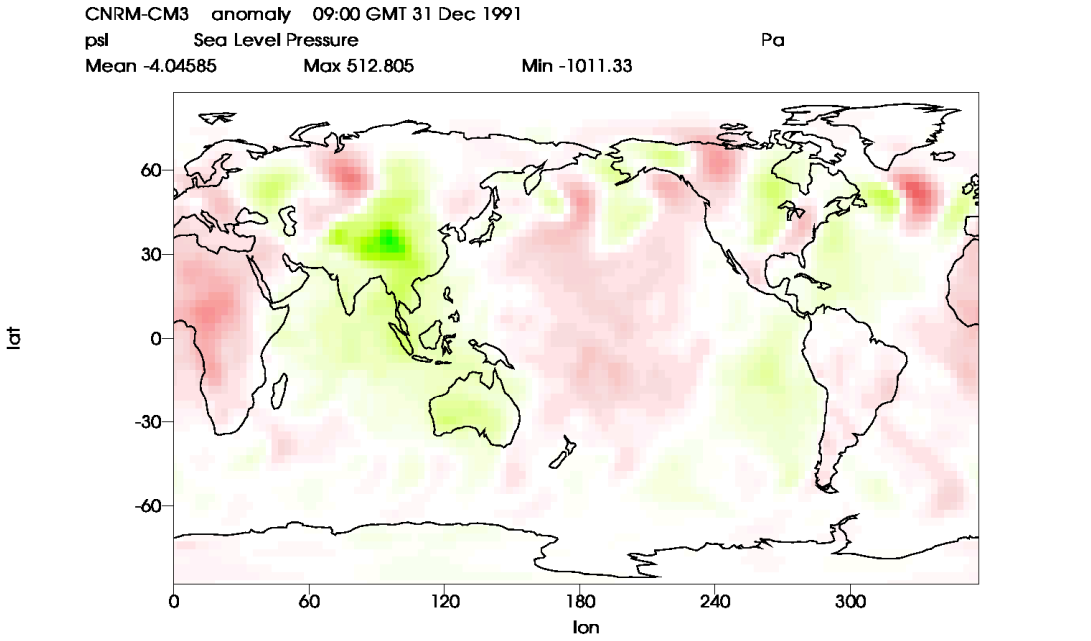
CNRM-CM3 anomaly 09:00 GMT 31 Dec 1991
psl Sea Level Pressure Pa
Mean -4.04585 Max 512.805 Min -1011.33
lat
60
30
0
-30
-60
0
60
120
180
240
300
lon
-2000
-1600
-1200
-800
-400
0
400
800
1200
1600
2000

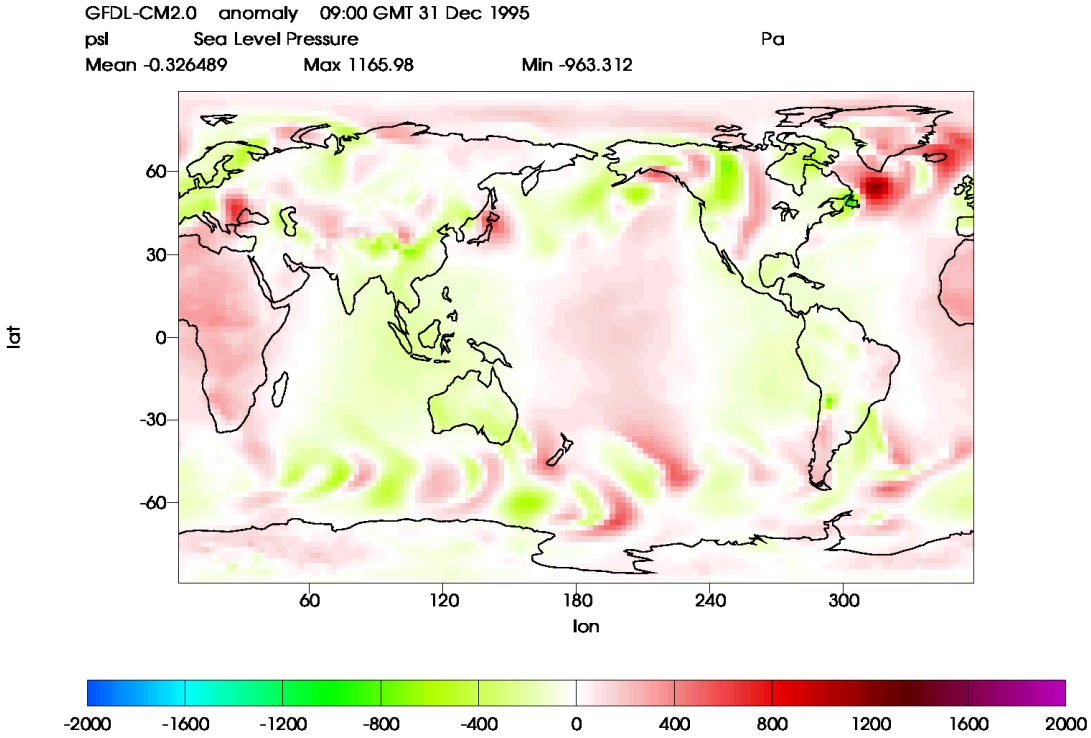
GFDL-CM2.0 anomaly 09:00 GMT 31 Dec 1995
psl Sea Level Pressure Pa
Mean -0.326489 Max 1165.98 Min -963.312
lat
60
30
0
-30
-60
60
120
180
240
300
lon
-2000
-1600
-1200
-800
-400
0
400
800
1200
1600
2000

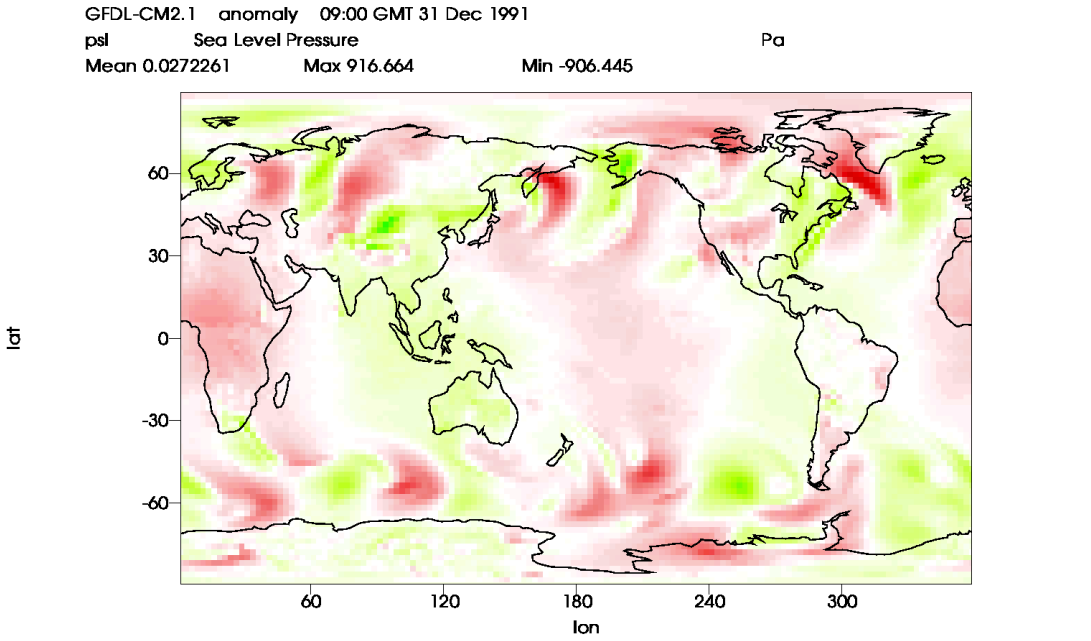
GFDL-CM2.1 anomaly 09:00 GMT 31 Dec 1991
psl Sea Level Pressure Pa
Mean 0.0272261 Max 916.664 Min -906.445
lat
60
30
0
-30
-60
60 120 180 240 300
lon
-2000 -1600 -1200 -800 -400 0 400 800 1200 1600 2000

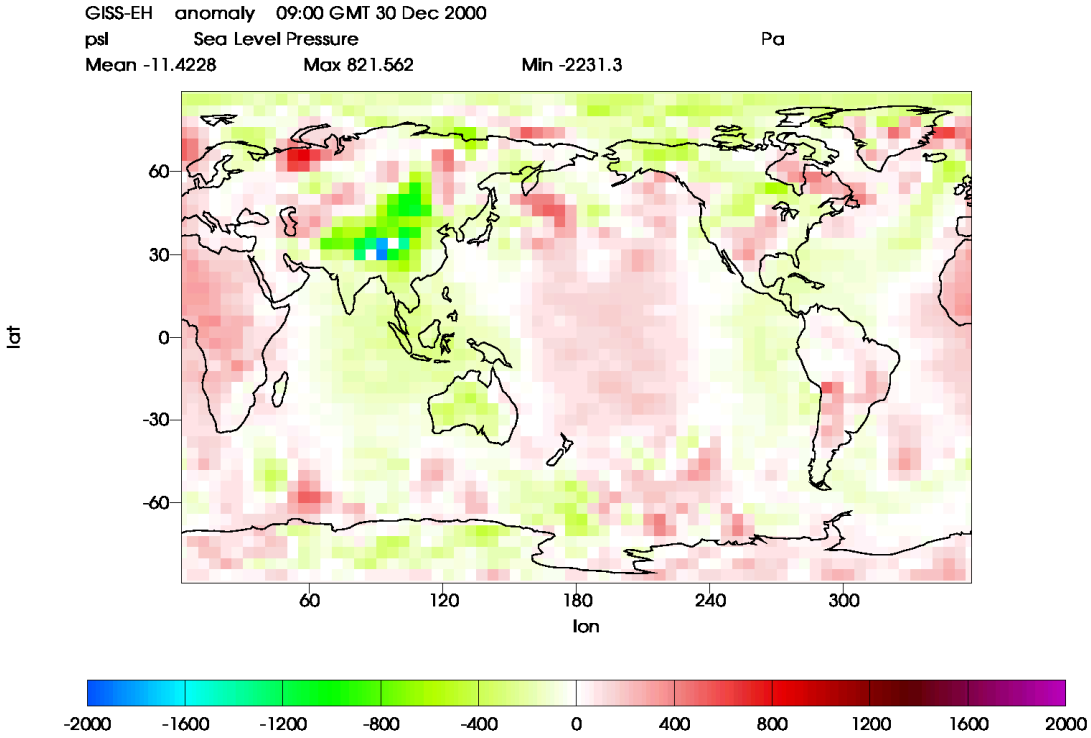
GISS-EH anomaly 09:00 GMT 30 Dec 2000
psl Sea Level Pressure Pa
Mean -11.4228 Max 821.562 Min -2231.3
lat
60
30
0
-30
-60
60 120 180 240 300
lon
-2000 -1600 -1200 -800 -400 0 400 800 1200 1600 2000

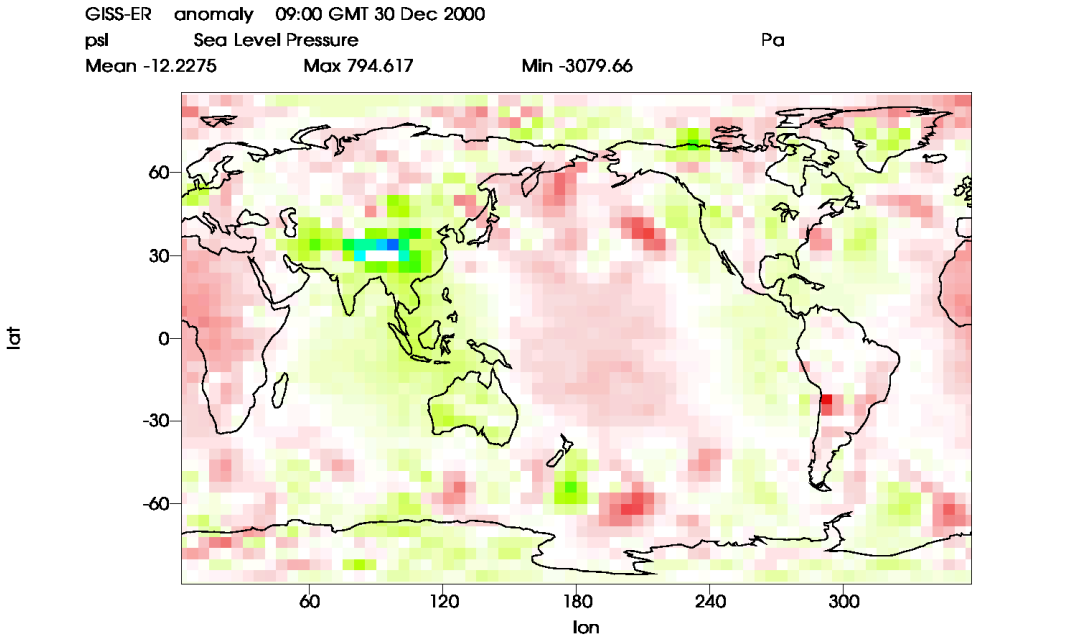
GISS-ER anomaly 09:00 GMT 30 Dec 2000
psl Sea Level Pressure Pa
Mean -12.2275 Max 794.617 Min -3079.66
lat
60
30
0
-30
-60
60 120 180 240 300
lon
-2000 -1600 -1200 -800 -400 0 400 800 1200 1600 2000

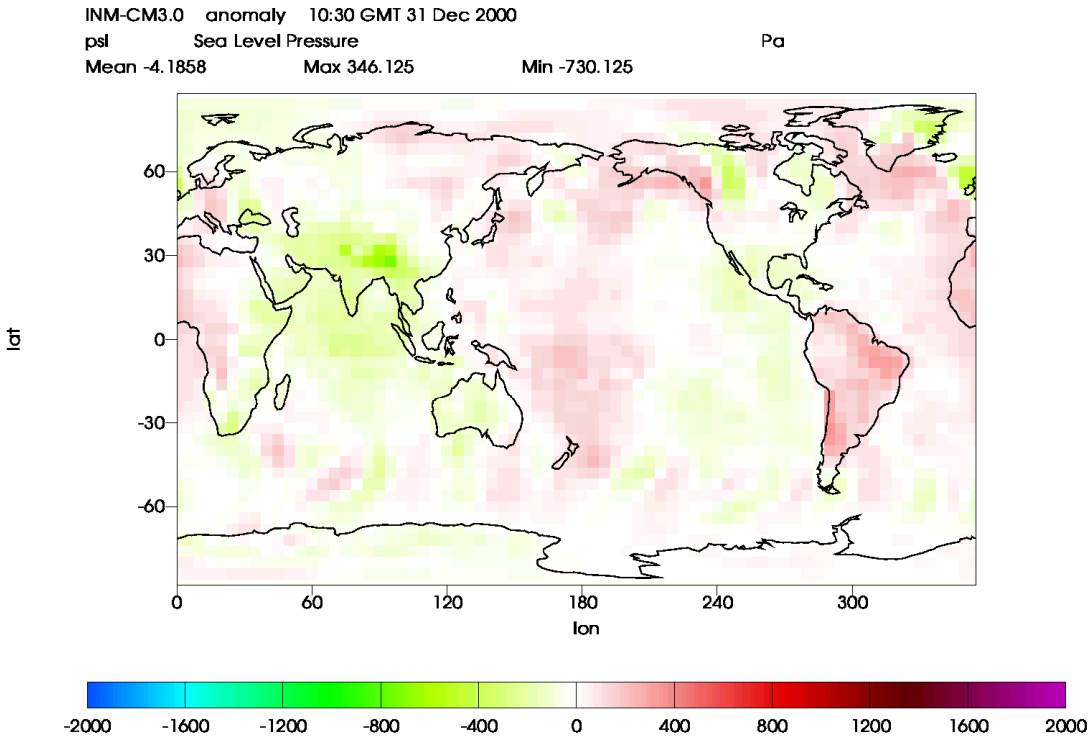
INM-CM3.0 anomaly 10:30 GMT 31 Dec 2000
psl Sea Level Pressure Pa
Mean -4.1858 Max 346.125 Min -730.125
lat
60
30
0
-30
-60
0 60 120 180 240 300
lon
-2000 -1600 -1200 -800 -400 0 400 800 1200 1600 2000

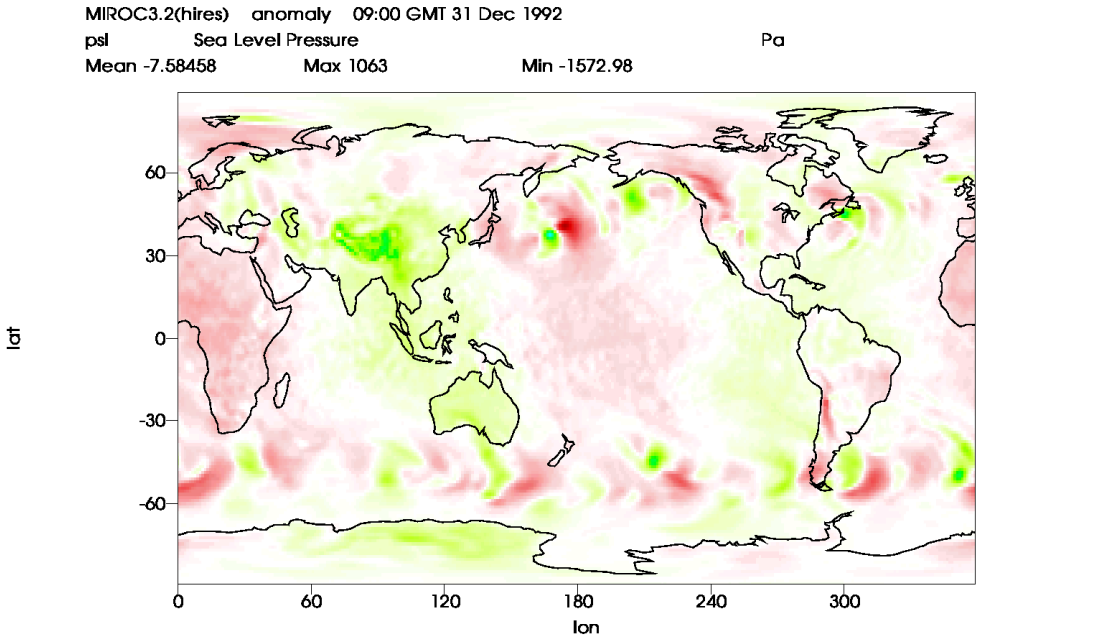
MIROC3.2(hires) anomaly 09:00 GMT 31 Dec 1992
psl Sea Level Pressure Pa
Mean -7.58458 Max 1063 Min -1572.98
lat
60
30
0
-30
-60
0
60
120
180
240
300
lon
-2000
-1600
-1200
-800
-400
0
400
800
1200
1600
2000

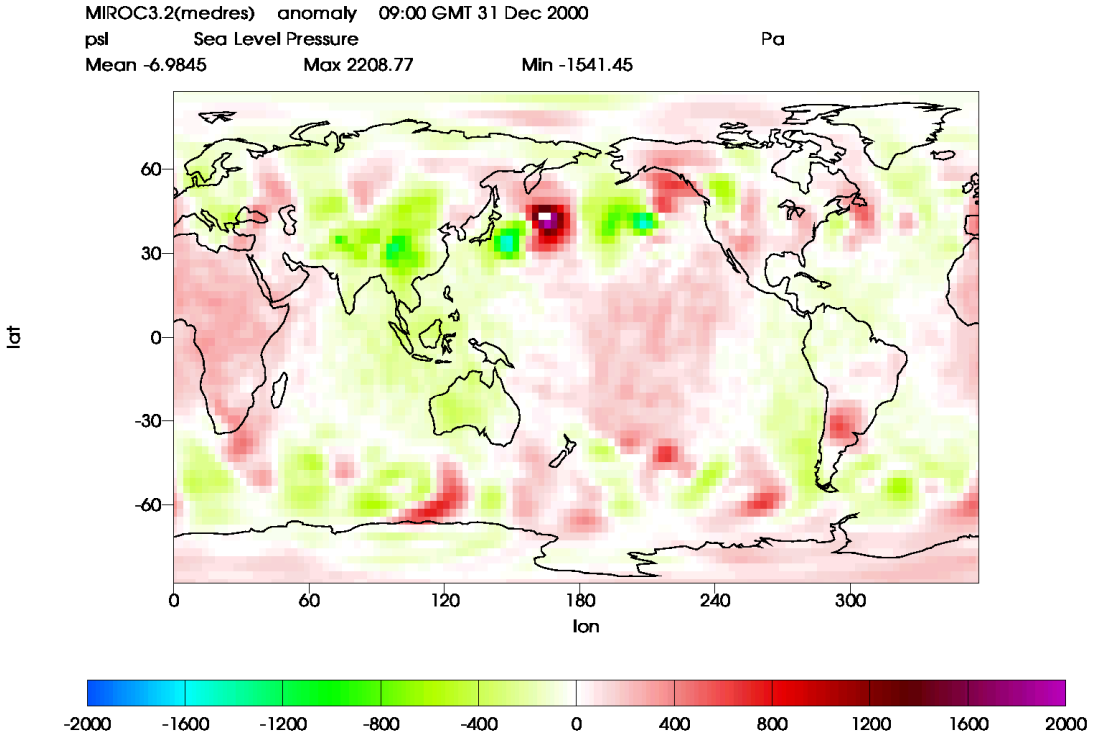
MIROC3.2(medres) anomaly 09:00 GMT 31 Dec 2000
psl Sea Level Pressure Pa
Mean -6.9845 Max 2208.77 Min -1541.45
lat
60
30
0
-30
-60
0
60
120
180
240
300
lon
-2000
-1600
-1200
-800
-400
0
400
800
1200
1600
2000

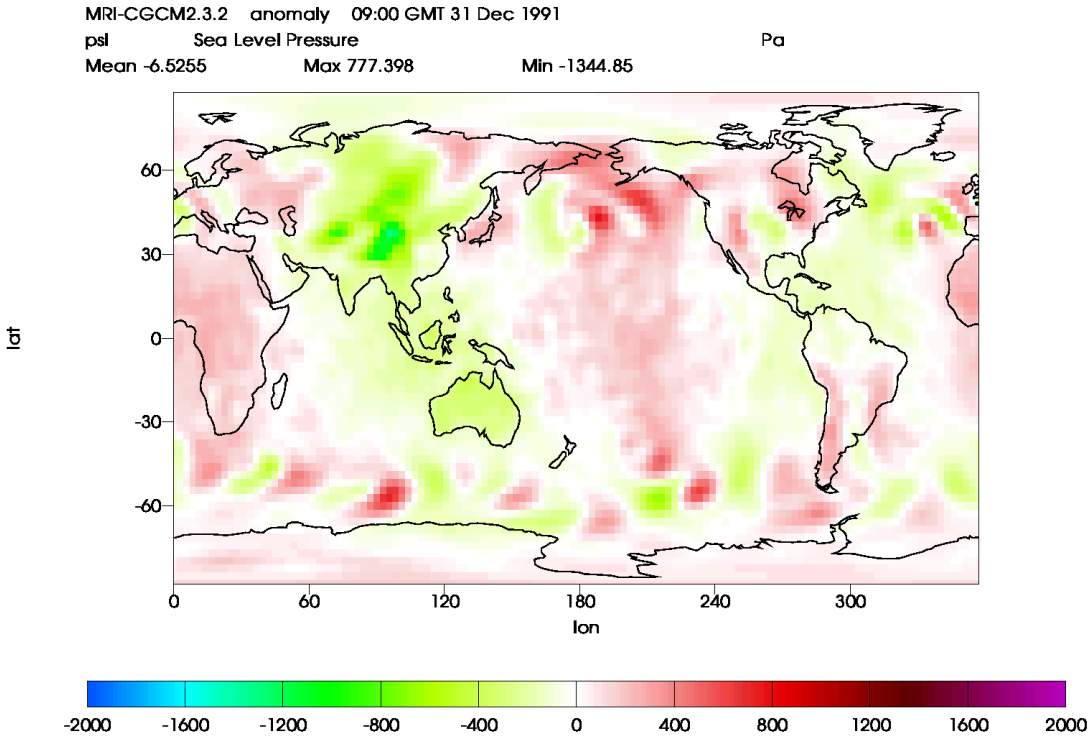

All maps are snapshots at 9 AM GMT except for the INM-CM3.0 map, which is a snapshot at 10:30 AM GMT. All exhibit a low-latitude wavenumber-2 disturbance maximizing at around 10 AM and PM local solar time, in agreement with the observations (cf. Figure 2 of Dai and Wang 1999, and Figure 4 of Dai and Trenberth 2004). Because the maps above are differences between instantaneous snapshots and corresponding daily means, they also show residuals of baroclinic waves at middle latitudes.

The resemblance of the maps to each other—and to the observations—is at first sight surprising. The CMIP3 / IPCC models were designed to simulate large-scale weather patterns and global climate change, not atmospheric tides. One might think that since the tides are a linear response to known forcing, simulation of them would happen automatically in a comprehensive GCM, but it was not clear to us at the outset of this project that the CMIP3 / IPCC models included all of the relevant forcing or the ability to transmit it to the surface. The models differ not only in their horizontal resolution (apparent in the smoothness or lack of it in the graphics above) but also in their vertical domain and resolution, as noted in the table above. Two of the models have “tops” at about the 10 mbar pressure level (~30 km altitude), omitting most of the stratosphere. Among the other models, the number of levels in the stratosphere ranges from 4 to 22. Classical tidal theory (Chapman and Lindzen 1970) and current opinion has at least half of the migrating semidiurnal surface-pressure tide forced by stratospheric ozone heating. Downward gravity wave propagation transmits the signal to the surface; this propagation is more efficient for the semidiurnal than the diurnal harmonic of the ozone forcing. The

remainder of the semidiurnal tide forcing, and most of the diurnal tide forcing, arises in the lower atmosphere from solar energy absorption by water vapor and daily variation in convective rainfall.

From these considerations one might expect the CMIP3 / IPCC models with tops at ~10 mbar to omit much of semidiurnal tide forcing, and the models with poorer stratospheric resolution to have more difficulty propagating it to the surface. Indeed, examination of ozone at altitudes below the 10-mbar pressure level reveals all of the models using the same amounts (not shown; note also that the CMIP3 database does not include radiative heating or ozone amounts for $p < 10$ mbar). Thus, the two models with a top at 10 mbar do not artificially compensate for their missing ozone heating by increasing it at or below this level. Nevertheless these models—and the ones with a stratosphere represented only at crude vertical resolution—appear to simulate surface-pressure tides with comparable fidelity to models with a more complete middle atmosphere, including WACCM.*

More complete analysis of surface-pressure tides in the CMIP3 / IPCC models must confront the limitation noted above in the CMIP3 database. In future work we will attempt to reconstruct high-frequency surface pressure from high-frequency sea level pressure in this database.

* A model top at 10 mbar could artificially reflect upward-propagating gravity waves downward, spuriously enhancing the semidiurnal tide at the surface and thereby making up for the lack of ozone forcing at altitudes above the 10-mbar pressure level. This type of potential problem with GCM simulations of the tides has long been recognized (Lindzen et al. 1968). It would be pure speculation at this point, however, to attribute it to any of the models considered here.

REFERENCES

Chapman, S., and R. S. Lindzen, 1970: Atmospheric Tides, D. Reidel, 200 pp.

Dai, A., and J. Wang, 1999: Diurnal and Semidiurnal Tides in Global Surface Pressure Fields, Journal of the Atmospheric Sciences, 56, 3874-3890

Dai, A., and K. E. Trenberth, 2004: The Diurnal Cycle and its Depiction in the Community Climate System Model, Journal of Climate, 17, 930-951

Hagan, M. E., J. M. Forbes and A. Richmond, 2003: Atmospheric Tides, in the Encyclopedia of Atmospheric Sciences, ed. J. R. Holton, Academic Press

Lindzen, R.S., E.S. Batten and J.-W. Kim, 1968: Oscillations in atmospheres with tops, Monthly Weather Review 96: 133-140

Meehl, G.A, C. Covey, T. Delworth, M. Latif, B. McAvaney, J.F.B. Mitchell, R.J. Stouffer and K.E. Taylor, 2007: The WCRP CMIP3 multimodel dataset: A new era in climate change research, Bulletin of the American Meteorological Society, September 2007 issue, pp. 1383-1394

Randall, D.A., R.A. Wood, S. Bony, R. Colman, T. Fichefet, J. Fyfe, V. Kattsov, A. Pitman, J. Shukla, J. Srinivasan, R.J. Stouffer, A. Sumi and K.E. Taylor, 2007: Climate Models and Their Evaluation. In: Climate Change 2007: The Physical Science Basis. Contribution of Working Group I to the Fourth Assessment Report of the Intergovernmental Panel on Climate Change [Solomon, S., D. Qin, M. Manning, Z. Chen, M. Marquis, K.B. Averyt, M.Tignor and H.L. Miller (eds.)]. Cambridge University Press, Cambridge, United Kingdom and New York, NY, USA

Richter, J., F. Sassi, R.R. Garcia, K. Matthes, and C.A. Fischer, 2008: Dynamics of the middle atmosphere as simulated by the Whole Atmosphere Community Climate Model, version 3 (WACCM3), Journal of Geophysical Research, in press

Sassi, F.S., R.R. Garcia, B.A. Boville, and H. Liu, 2002: On temperature inversions and the mesospheric surf zone, Journal of Geophysical Research 107 (D19), 4380, doi: 10.1029/2001JD001525